The Journal of Physical Chemistry A

 VOLUME 102, NUMBER 30, JULY 23, 1998

ARTICLES

Trajectory Surface Hopping Study of the Li + $Li_2(X^1\Sigma_g^+)$ Dissociation Reaction

A. I. Voronin, J. M. C. Marques, and A. J. C. Varandas*

Departamento de Química, Universidade de Coimbra, P-3049 Coimbra Codex, Portugal

Received: December 19, 1997; In Final Form: March 13, 1998

Trajectory surface hopping calculations are reported for the Li + $Li_2(X^1\Sigma_g^+)$ dissociation reaction over the range of translational energies $13 \leq E_{tr}$/kcal mol$^{-1} \leq 80$. Both potential energy surfaces for ground doublet Li_3, which have been modeled from the double many-body expansion method (DMBE III), have been employed in the dynamics calculations. For the initial internal state ($v = 0$, $j = 10$), the behavior of the dissociative cross sections as a function of translational energy shows that nonadiabatic effects are important over the whole range of energies studied. Concerning the role of initial vibration, it has been found that, for $E_{tr} = 25$ kcal mol^{-1} and $j = 10$, the adiabatic dissociative cross sections are enhanced as v increases from 0 to 20, while the nonadiabatic ones just slightly increase with the vibrational quantum number.

1. Introduction

The study of nonadiabatic chemical reactions demanding the knowledge of two or more electronic states has received a great deal of attention in recent years, both experimental and theoretical. The most important cases for reaction dynamics arise when two potential energy surfaces have conical intersections at some specific internuclear configurations. As a result of such intersections, the standard Born−Oppenheimer approximation needs to be modified to take into account the nonadiabatic interactions between the involved potential energy surfaces. Indeed, it has become apparent that nonadiabatic effects can play a significant role in the dynamics of many chemical reactions, and hence the restriction of using only one potential energy surface may not be valid.

The simplest systems which exhibit a conical intersection between the two lowest potential energy surfaces are H_3[1] and the alkali metal trimers such as Li_3 and Na_3.[2,3] The existence of conical intersections for these systems can provide a new mechanism for collision-induced chemical reactions, in particular, for the dissociation processes. Although there have been many calculations on exchange chemical reactions[4] that account for nonadiabatic effects, the role of conical intersections on collision-induced dissociation has been the subject of only two studies[5,6] both for the H + $H_2(v,j)$ system. This is partly due to the fact that such studies demand the availability of accurate potential energy surfaces including a correct description of the dissociation limits, a very difficult task in itself.

Recently,[7,8] a realistic two-valued semiempirical potential energy surface has been reported for Li_3, which is based on the double many-body expansion[9,10] (DMBE) method and takes into account the normalization of the kinetic field.[11] (This version of the Li_3 potential energy surface has been, and will be henceforward, referred to as DMBE III.) In comparison with previous LEPS-type forms,[12,13] the Li_3 DMBE III potential energy surface has the advantage of properly describing the D_{3h} conical intersection which is localized well below the dissociation limit for Li + Li + Li. Thus, it can be used for dynamics studies of the collision-induced Li + $Li_2(X^1\Sigma_g^+)$ dissociation or the exchange reactions by quasiclassical or quantum mechanical methods. It should be noted that the exchange reactions of alkali atoms and molecules M′ + $M_2(v,j)$ (M, M′ = Li, Na, K, Rb, Cs) have been much studied from both the experimental and theoretical points of view.[14−18] In turn, the DMBE III potential energy surface has previously been employed for adiabatic studies[19] of the Li + Li_2 exchange reaction and most

S1089-5639(98)00586-6 CCC: $15.00
Published on Web 07/03/1998

recently[20] for quantum calculations of the Li_3 vibrational levels both with consideration and without consideration of the so-called geometric phase effect (for a recent review on this nonadiabatic effect which refers to earlier work, see ref 21). A major motivation for such an interest is the fact that the alkali metal atom−alkali metal dimer reactions are believed to occur on barrierless potential energy surfaces, and hence they provide important prototypes of reactions controlled by long-range dispersion forces. Furthermore, alkali metal trimers are convenient systems for experimental studies due to the possibility of vibrational excitation in the visible and near-infrared regions, for which proper tunable lasers are available.

In this work, we report an investigation by the trajectory surface hopping[4,22,23] (TSH) method of the adiabatic and nonadiabatic Li + $Li_2(v,j)$ dissociative channels and the effects of the D_{3h} conical intersection on such processes, which can be either direct or indirect. In this case, the conical intersection manifests through symmetry effects associated with the nonuniqueness of the electronic wave functions (refs 20, 21, and references therein) and hence will be of no concern to us in the present work. Direct effects may in turn arise when the trajectories sample both intersecting adiabatic potential energy surfaces and hence can be observed in the present work. Specifically, we focus on this study on the energy dependence of the dissociative cross sections for the adiabatic and nonadiabatic channels, i.e., when reaction takes place on the lower and upper sheets of the two-valued DMBE III potential energy surface, respectively. Moreover, we examine the role of vibrational excitation on the dissociative process and study the energy dependence of the exchange reaction probability on the ground adiabatic potential energy surface.

A few comments concerning the TSH method of Tully and Preston,[22,29] which is used for the present dynamics calculations, are appropriate at this point. First, we note that its adequacy for describing nonadiabatic effects has been the subject of many studies including applications to concrete chemical systems (e.g., refs 24−26). Additionally, we observe that the TSH method has been shown to underestimate the relevant nonadiabatic transition probabilities when compared with the exact quantum results.[27] Indeed, such a conclusion has also been derived from past experience in low-dimensional systems.[28] Conversely, the TSH method has been recognized to be quite accurate for collision-induced dissociation studies in the H + $H_2(v,j)$ system.[6] Of course, as noted by Tully and Preston,[22,29] their method requires for accuracy that the Landau−Zener formula is valid to describe the diabatic curves (i.e., these curves should look fairly linear in the vicinity of the crossing seam). Moreover, the derivative coupling terms should be nearly constant in the hopping regions. Although there are methods for treating the hopping that rely on a semiclassical propagation of the electronic populations[4,30−33] and are particularly useful for treating more than three atoms, such methods are not free from problems. In fact, the determination of the nonadiabatic terms along a trajectory is not easy, especially if we have only the intersecting adiabatic potential energy surfaces, as is the case in the present work. Our approximation seems therefore legitimate and will hopefully lead to reasonable results for the Li + $Li_2(v,j)$ dissociation process that we study here.

The plan of the paper is as follows. In section 2 we discuss the methodology and main topographical features of the potential energy surface for the Li_3 system. Section 3 describes the necessary technical specifications, while section 4 contains the results and discussion. The major conclusions are in section 5.

2. Methodology and Potential Energy Surface

As pointed out in the Introduction, we have adopted to describe the dynamics of the dissociation reaction Li + $Li_2(X^1\Sigma_g^+) \rightarrow$ Li + Li + Li with the quasiclassical TSH method proposed by Tully and Preston.[22] According to their prescription, each trajectory is governed at the beginning by the ground adiabatic potential energy surface $V_1(\mathbf{R})$; $\mathbf{R} = (R_1,R_2,R_3)$ denotes the full set of internuclear coordinates. After each integration step we then examine the difference $\Delta V_{12} = V_2 - V_1$ between the two sheets of the potential energy surface along the trajectory path. Whenever ΔV_{12} reaches a minimum value, the trajectory will be halted and the values of V_1 and V_2 at the three last points used to calculate the parameters of the Landau−Zener formula for the probability of nonadiabatic transition

$$P_{LZ} = \exp(-2\pi A^2/\hbar B u) \tag{1}$$

In eq 1, u is the velocity, and A and B are the parameters that define the splitting between V_1 and V_2 at the instant t given by

$$\Delta V_{12} = [B^2u^2(t-\tau)^2 + 4A^2]^{1/2} \tag{2}$$

where τ is the time corresponding to the minimum of ΔV_{12}. Since we have to decide on which sheet of the potential energy surface the trajectory is going to proceed, a random number ξ is generated and compared with the surface hopping probability of eq 1. If $P_{LZ} < \xi$, the trajectory continues on the same potential energy surface. Conversely, if $P_{LZ} \geq \xi$, we allow the trajectory to hop on the other potential energy surface. Since $V_1 \neq V_2$ in general, the momenta on the new potential energy surface are adjusted according to the procedure suggested by Tully and Preston,[22] while the coordinates are kept unchanged during the hop. This approximation warrants conservation of both energy and momenta.

We now turn to describe the main features of the two-valued potential energy surface for Li_3 used in the present work. This potential energy surface, DMBE III, is based on the double many-body expansion method[9] and reproduces the experimental dissociation energy of Li_3. It also accurately describes the long-range behavior for all possible dissociation channels, while satisfying the virial theorem restrictions through proper parametrization of the involved two-body energy curves. Moreover, the DMBE III potential function conforms with existing three-body ab initio data at the valence region of the lowest sheet while predicting the atomization energy of Li_3 within the error limits of the experimental value. In addition, the dynamics studies of the Li + $Li_2(X^1\Sigma_g^+)$ exchange reaction based on the ground-state sheet alone[7,19] have shown good agreement with the experimentally determined behavior for similar systems, namely, an increase in the reactive cross sections with increasing vibrational quantum number v. Because the functional form has the correct analytic expression at the conical intersection, it also fits in a satisfactory way the available ab initio data[2] on the upper sheet for geometries in the vicinity of the D_{3h} conical intersection.

Since the details concerning the Li_3 DMBE III potential energy surface have been previously presented and discussed, we give here only the most important attributes with relevance in the adiabatic and nonadiabatic dynamics of the title reaction. Figure 1 shows a diagram of the energetics of the Li_3 DMBE III potential energy surface. It is seen that the dissociative channel is 24.35 kcal mol^{-1} above the classical minimum (i.e., without considering zero-point vibrational energy) of the reactants, but only 23.63, 14.36, and 6.89 kcal mol^{-1} when one

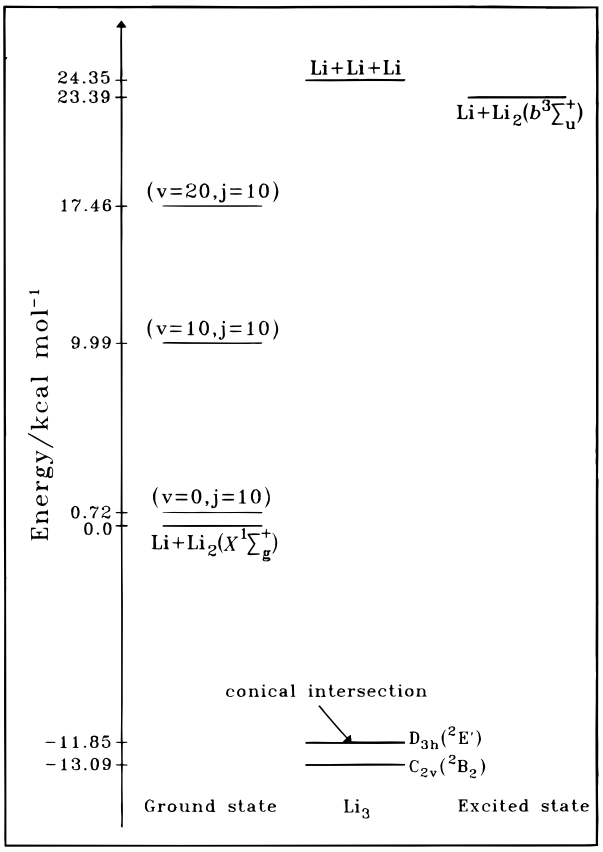

Figure 1. Schematic diagram of the energetics for the Li + $Li_2(X^1\Sigma_g^+)$ dissociation reaction.

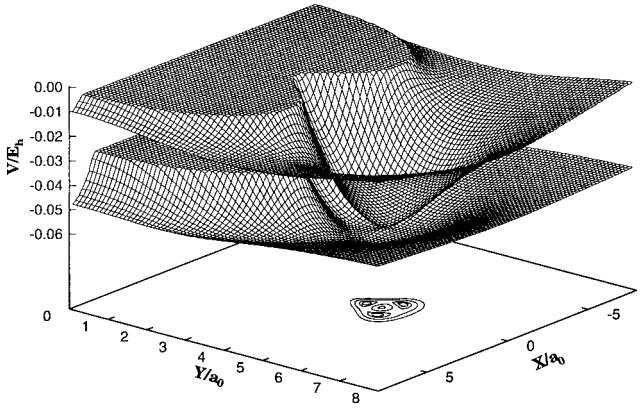

Figure 2. Perspective view of the two sheets of the Li_3 DMBE III potential energy surface for a lithium atom moving around a partially relaxed Li_2 diatomic ($4.5 \leq R_{Li-Li}/a_0 \leq 6.5$). The contours in the *XY* -plane refer to the ground-state sheet and illustrate the three equivalent minima and conical intersection.

considers the internal states ($v = 0$, $j = 10$), ($v = 10$, $j = 10$), and ($v = 20$, $j = 10$), respectively. Moreover, the conical intersection that arises for D_{3h} geometries has its lowest energy value localized at $R_1 = R_2 = R_3 = 5.465a_0$, i.e., 1.24 kcal mol^{-1} above the $C_{2v}(^2B_2)$ minima. In turn, Figure 2 shows a perspective plot of the lowest and upper sheets for a $Li(^2S)$ atom moving around a $Li_2(X^1\Sigma_g^+)$ molecule, the bond length of which is allowed to relax in the range $4.5 \leq R_{Li-Li}/a_0 \leq 6.5$. Note that the upper sheet correlates with the Li + $Li_2(b^3\Sigma_u^+)$ dissociation channel, with $Li_2(b^3\Sigma_u^+)$ being a van der Waals molecule that has a minimum ~0.97 kcal mol^{-1} deep at $R_{Li-Li} = 7.77\ a_0$.

3. Computational Details

The dynamics calculations have used our own computer code, which has its basis on an extensively adapted version of the Muckerman program[34] to include the TSH method of Tully and Preston[22] described in section 2. As usual, the determination of the integration time step has been done by trial and error in order to warrant that total energy and angular momentum are conserved with an error less than 10^{-6} atomic units for most trajectories. Only for a few of them has such an error been found to increase to 10^{-4} atomic units. In practice, a high level of accuracy has been reached by choosing a value of ~2.0 atu for all sets of initial conditions.

Batches of 5000 trajectories have been run for $E_{tr} = 25$, 27, 28.5, 30, 32.5, 35, 40, 45, 50, and 80 kcal mol^{-1} and internal state ($v = 0$, $j = 10$). As it has been pointed out,[7,19] the rotational quantum number $j = 10$ corresponds approximately to the most likely value in supersonic molecular beams[35] and hence has been adopted here for all calculations. We have also run 5000 trajectories for the low translational energy of 13.1 kcal mol^{-1} and $v = 20$, which is clearly above the dissociation threshold (see Figure 1). Moreover, using only the lowest sheet of the DMBE III potential energy surface, we have run batches of 5000 trajectories for $E_{tr} = 13.1$ kcal mol^{-1} ($v = 20$) and $E_{tr} = 25$ and 50 kcal mol^{-1} ($v = 0$ for both of them) to examine the role of the conical intersection in the title system. To study the effect of initial vibrational energy on the Li + Li_2 dissociation, we have run additional batches of 5000 trajectories for $E_{tr} = 25$ kcal mol^{-1}, but considering now the vibrational quantum numbers $v = 10$ and $v = 20$ for the reactant diatomic.

Since the main goal of the present work is the study of the reaction Li + $Li_2 \rightarrow$ Li + Li + Li, the corresponding maximum value of the impact parameter, b_{max}, has been optimized for each set of initial conditions by taking into account only the dissociative process, in both the lower and upper sheets of DMBE III. The values of b_{max} so obtained are shown in Table 1 for each translational energy and vibrational quantum number. For the remaining channels arising in the Li + Li_2 collisions we just refer to the reaction probability for the specific initial conditions.

Since the total energy of the collisional system is always above the D_{3h} conical intersection, it is possible to form products via the upper sheet as well as through the ground electronic state. Thus, for the title reaction, we have five different outcomes: nonreactive, and reactive and dissociative trajectories both in the lower and upper sheets. In the lower sheet the reactive events, named N_{exc}^{a} in Table 1, are associated with the two possibilities of exchanging the lithium atoms to form Li + $Li_2(X^1\Sigma_g^+)$ products, one of the atoms in the product diatomic being the free atom of the reactants. The reactive events in the upper sheet (N_r^{na} in Table 1) are those leading to formation of Li + $Li_2(b^3\Sigma_u^+)$ products, independently of the combination of lithium atoms to form the diatomic. For the dissociative channels leading to three separated atoms Li + Li + Li, we assume any contribution of quasibound states of Li_2 to be negligible in both the lower (N_{dis}^{a}) and upper (N_{dis}^{na}) sheets. Figure 3 shows two typical dissociative trajectories, one being adiabatic [panel a] without hops and the other nonadiabatic [panel b] with one hop, which is signaled by the arrow; note the increasing complexity of the dissociative dynamics introduced by the hop in the nonadiabatic trajectory. Finally, nonreactive trajectories are, of course, the only remaining events.

From the number of trajectories for the adiabatic (N_{dis}^{a}) and nonadiabatic (N_{dis}^{na}) dissociation, we have calculated the corresponding cross section by using the expression

TABLE 1: Summary of the Trajectory Calculations for the Li + $Li_2(X^1\Sigma_g^+)$ Reaction[a]

			lower sheet			upper sheet			
E_{tr}/kcal mol^{-1}	v	b_{max}/a_0	N_{dis}^a	N_{exc}^a	σ_d^a/a_0^2	N_{dis}^{na}	N_r^{na}	σ_d^{na}/a_0^2	$\sigma_{tot}{}^b/a_0^2$
13.1	20	14.70	759	1183	103.0 ± 3.4	74	7	10.0 ± 1.2	113.0 ± 3.6
		14.70	819	1261	111.2 ± 3.6				
25.0	0	5.70	59	1598	1.2 ± 0.2	108	102	2.2 ± 0.2	3.4 ± 0.3
		5.70	46	1694	0.9 ± 0.1				
	10	12.50	632	538	62.0 ± 2.3	115	17	11.3 ± 1.0	73.3 ± 2.5
	20	14.00	1320	469	162.6 ± 3.8	125	13	15.4 ± 1.4	178.0 ± 4.0
27.0	0	6.30	142	1157	3.5 ± 0.3	298	68	7.4 ± 0.4	11.0 ± 0.5
28.5	0	6.35	201	1097	5.1 ± 0.4	323	56	8.2 ± 0.4	13.3 ± 0.6
30.0	0	6.50	241	940	6.4 ± 0.4	369	42	9.8 ± 0.5	16.2 ± 0.6
32.5	0	6.50	319	868	8.5 ± 0.5	345	35	9.2 ± 0.5	17.6 ± 0.6
35.0	0	6.40	402	810	10.3 ± 0.5	376	23	9.7 ± 0.5	20.0 ± 0.7
40.0	0	6.25	582	706	14.3 ± 0.6	402	20	9.9 ± 0.5	24.2 ± 0.7
45.0	0	6.20	717	647	17.3 ± 0.6	397	9	9.6 ± 0.5	26.9 ± 0.7
50.0	0	6.10	830	577	19.4 ± 0.6	421	9	9.8 ± 0.5	29.2 ± 0.7
		5.70	1076	774	22.0 ± 0.6				
80.0	0	5.80	1220	335	25.8 ± 0.6	511	1	10.8 ± 0.4	36.6 ± 0.7

[a] For E_{tr} = 13.1 kcal mol^{-1} (v = 20), E_{tr}= 25 and 50 kcal mol^{-1} (both v = 0), the second entry refers to the trajectory calculations where only the lower sheet of the DMBE III potential energy surface was considered. [b] Note that σ_{tot} is the total dissociative cross section, in both the lower and upper sheets.

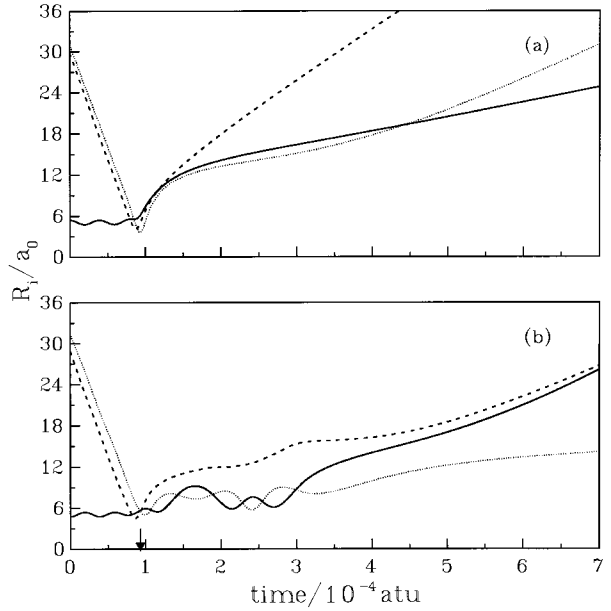

Figure 3. Typical surface hopping trajectories leading to dissociation via lower sheet [panel a] and upper sheet [panel b]. The arrow indicates the hop occurring along the trajectory. Note that the three distances become large at the end of the trajectories.

$$\sigma_d^x = \pi b_{max}^2 \frac{N_{dis}^x}{N} \tag{3}$$

where N = 5000 trajectories and x stands for the superscripts a or na. Moreover, the 68% standard error is given by

$$\Delta\sigma_d^x = \sigma_d^x \left(\frac{N - N_{dis}^x}{N N_{dis}^x} \right)^{1/2} \tag{4}$$

Table 1 shows the dissociative cross sections σ_d^a (column six) and σ_d^{na} (column nine), together with the corresponding $\Delta\sigma_d$. The total dissociative cross sections $\sigma_{tot} = \sigma_d^a + \sigma_d^{na}$ are given in column 10. To get an indication of the influence of conical intersection on the dynamics of the title reaction, we have also computed the number of hops occurring along the trajectory. Note that an even total number of hops arising in a dissociative trajectory implies that, although it has evolved during sometime in the upper sheet, the elemental process Li + Li_2 → Li + Li + Li occurred via the ground electronic state of DMBE III; that is, it ended in the lower sheet. Conversely, the dissociative reaction occurs via the upper sheet if the number of hops is odd. In Table 2 we distribute the total number of dissociative trajectories by sets of those ending in the lower sheet with 0, 2, 4, 6, and 8 hops or in the upper sheet with 1, 3, 5, and 7 hops. The results presented in both Tables 1 and 2 are discussed in section 4.

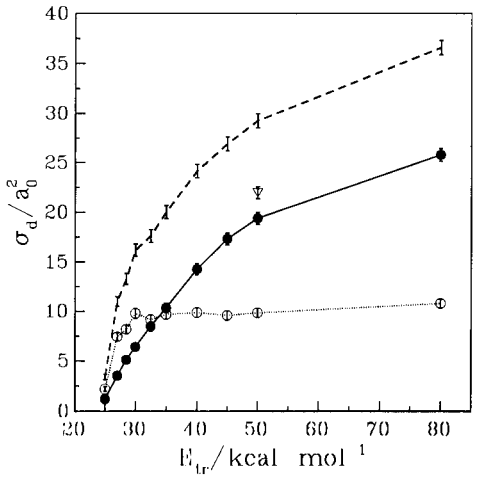

Figure 4. Dissociative cross sections for the title reaction as a function of initial translational energy. For calculations involving the two sheets: (— and ●) adiabatic dissociation; (··· and ○) nonadiabatic dissociation; (- - -) total dissociative process. For calculations involving only the lowest sheet at E_{tr} = 25 and 50 kcal mol^{-1}: (▽) dissociation.

4. Results and Discussion

The role of the conical intersection in the Li + Li_2 dissociation reaction has been studied in the range of translational energies 13 ≤ E_{tr}/kcal mol^{-1} ≤ 80. Additionally, the effect of initial vibrational quantum number on the title reaction has been investigated.

Table 1 reports the values of the dissociative cross sections, while Figure 4 shows σ_d as a function of translational energy for v = 0. It is seen from Figure 4 that the total cross section (σ_{tot}) for Li + Li_2 dissociation always increases as the translational energy increases. However, it is clear from a more

TABLE 2: Distribution of Trajectories According to the Number of Hops Occurring during the Dissociative Process in the Lower Sheet (with Even Number of Hops) and the Upper Sheet (with Odd Number of Hops) for Each Set of Initial Conditions

E_{tr}/		even number of hops					odd number of hops			
kcal mol^{-1}	v	N_0	N_2	N_4	N_6	N_8	N_1	N_3	N_5	N_7
13.1	20	741	18	0	0	0	57	16	1	0
25.0	0	43	11	3	1	1	76	27	4	1
	10	618	13	1	0	0	89	26	0	0
	20	1303	17	0	0	0	105	20	0	0
27.0	0	111	28	3	0	0	251	46	1	0
28.5	0	180	21	0	0	0	278	40	5	0
30.0	0	228	13	0	0	0	307	62	0	0
32.5	0	303	16	0	0	0	292	53	0	0
35.0	0	384	18	0	0	0	314	61	1	0
40.0	0	546	36	0	0	0	345	57	0	0
45.0	0	673	44	0	0	0	335	59	3	0
50.0	0	785	45	0	0	0	363	56	2	0
80.0	0	1162	58	0	0	0	422	84	5	0

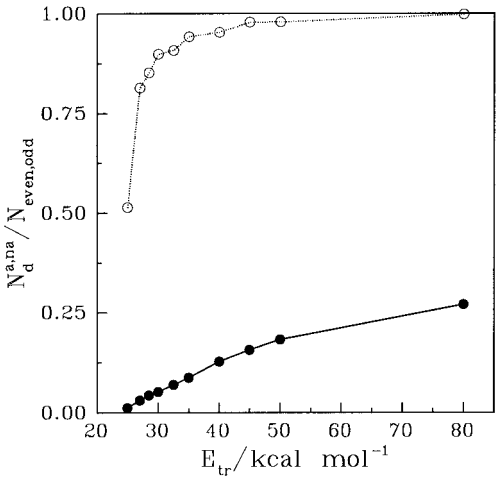

Figure 5. Efficiency for dissociation via lower sheet (●, —) and upper sheet (○, ···). See the text.

detailed observation of Figure 4 that, for energies just above the dissociation threshold, the nonadiabatic contribution to the title reaction is larger than the adiabatic one. This trend differs from that predicted for H + H_2 dissociation, where the calculated nonadiabatic cross sections are always below the adiabatic ones.[6] Additionally, Figure 4 shows that dissociation via the upper sheet increases sharply up to $E_{tr} = 30$ kcal mol^{-1}, which is due not only to the fast increase in b_{max} but also to the rise of the number of trajectories that, proceeding via the upper sheet, lead to dissociation. This increase in efficiency of the nonadiabatic dissociation (N_d^{na}/N_{odd}) is evident from Figure 5 and can be related to the fact that the other possible outcomes are associated with the weak $Li_2(b^3\Sigma_u^+)$ van der Waals molecule, which promptly dissociates as the energy increases. In contrast, the rate of variation in the efficiency of dissociation via the lower sheet (N_d^a/N_{even}) is slower, since the competitive channels lead to the more stable $Li_2(X^1\Sigma_g^+)$ product molecule; see Figure 1. Also important is the large reaction exchange probability plotted in Figure 6, which competes with all other channels, especially with that associated with adiabatic dissociation. In fact, Figure 6 shows that the exchange reaction probability is larger than the probability for other channels, being the dominant process particularly for translational energies just above the dissociation threshold.

As the translational energies increase for values higher than 30 kcal mol^{-1}, the nonadiabatic dissociative cross section keeps approximately constant at the value $\sigma_d^{na} \approx 10\ a_0^2$ or just

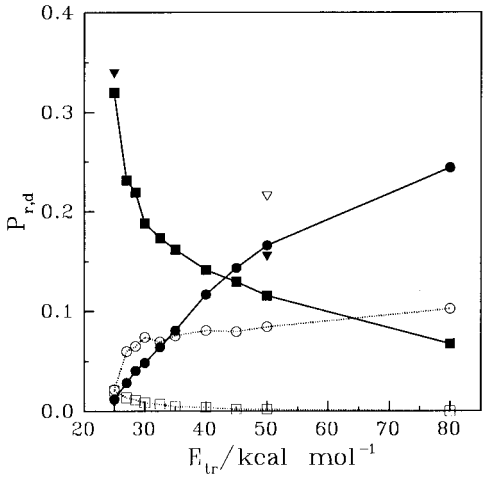

Figure 6. Reactive and dissociative probabilities for the Li_3 system as a function of initial translational energy. Calculations involving the two sheets: (—) processes occurring via lower sheet; (···) processes occurring via upper sheet; (●) adiabatic dissociation; (■) exchange reaction; (○) nonadiabatic dissociation; (□) reaction to form Li + $Li_2(b^3\Sigma_u^+)$ products. Calculations involving only the lowest sheet at $E_{tr} = 25$ and 50 kcal mol^{-1}: (▽) dissociation; (▼) exchange reaction.

slightly increases. Conversely, dissociation via the lower sheet always increases with increasing translational energy, becoming larger than the nonadiabatic one for $E_{tr} \sim 35$ kcal mol^{-1}. These trends can be understood from Figure 5, where it is shown that for high energies the efficiency for nonadiabatic dissociation tends to its maximum value of 1, while the efficiency for adiabatic dissociation always increases with approximately the same rate. Note that, for high energies, the exchange reaction becomes less important since its probability decreases slowly and is clearly below the probability of dissociation via the lower sheet, as displayed in Figure 6. On the other hand, for this high-energy regime the trend of the nonadiabatic dissociative cross section results from a subtle balance between the slight increase in the corresponding probability, due to the increase of the hopping probability (note from Table 2 that the total number of hops increases for high energies), and the small deacrease in maximum impact parameter.

Figure 4 shows also the dissociative cross sections obtained from the trajectory calculations for $E_{tr} = 25$ and 50 kcal mol^{-1} ($v = 0$) using only the lowest sheet of DMBE III. Additionally, we report in Table 1 a similar calculation for $E_{tr} = 13$ kcal mol^{-1} and $v = 20$ (second entry). It is clear from these results that the nonadiabatic dynamics has a minor influence at such low translational energies, as it could be anticipated by consideration of the surface hopping probabilities. Indeed, we conclude from eq 1 that the probability of hopping increases as the velocity increases and hence as E_{tr} increases. This result is confirmed by the number of trajectories against the number of hops shown in Table 2. In contrast, as E_{tr} increases to 50 kcal mol^{-1}, the dissociative dynamics is notably influenced by the presence of the conical intersection. Indeed, the dissociative cross section obtained by considering only the lower surface is significantly below σ_{tot}. This result is clearly due to the nonadiabatic contribution to dissociation. Thus, the conical intersection opens a new route for the reactive flux. Because the new arising channels can compete with the adiabatic ones, σ_d^a becomes smaller than the dissociative cross section obtained from the one-sheet calculation.

To study the influence of initial vibrational quantum number on the title reaction, we have plotted the dissociative cross sections against v in Figure 7; the corresponding numerical

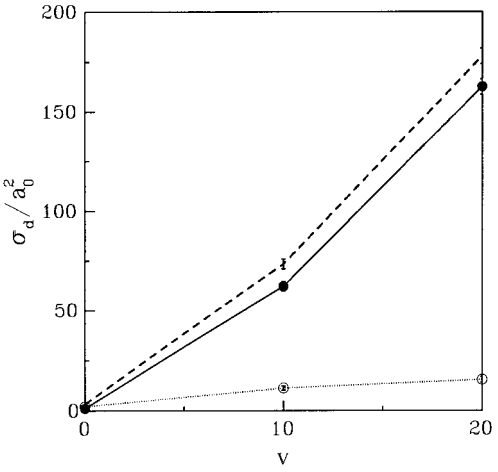

Figure 7. Dissociative cross sections for $E_{tr} = 25$ kcal mol^{-1} as a function of the initial vibrational quantum number v: (— and ●) adiabatic dissociation; (··· and ○) nonadiabatic dissociation; (- - -) total.

values are given in Table 1. We conclude from Figure 7 and Table 1 that total dissociative cross sections, σ_{tot}, definitely increases as v increases (and hence when the reactant diatomic is more stretched at the beginning of the trajectory). Indeed, since Li_2 is most likely to be dissociated as the Li atom approaches it, the reaction leading to Li + Li + Li via the lower sheet tends to be naturally favored. This behavior is shown in Figure 7 for σ_d^a as a function of v. Coversely, σ_d^{na} just slightly increases with the initial vibrational quantum number. Since the mechanism described above clearly favors the adibatic dissociation, we expect the small increase of σ_d^{na} to be due in this case to the rise of the surface hopping probability. In fact, this is corroborated from Table 2 by the growth of the number of trajectories with a larger number of hops as v increases from 0 to 20.

5. Final Remarks

We have reported the first trajectory surface hopping calculations for the Li + $Li_2(X^1\Sigma_g^+)$ dissociation reaction using a realistic two-valued DMBE potential energy surface. They have shown that the nonadiabatic dissociation channel plays an important role even at relatively low translational energies. Thus, nonadiabatic effects should be taken into account in any theoretical study of the collision-induced dissociation process involving this and other alkali metal trimeric systems.

Acknowledgment. The financial support from Fundação para a Ciência e Tecnologia, Portugal, is gratefully acknowledged.

References and Notes

(1) Porter, N.; Stevens, R. M.; Karplus, M. *J. Chem. Phys.* **1968**, *49*, 5163.

(2) Gerber, W. H.; Schumacher, E. *J. Chem. Phys.* **1978**, *69*, 1692.

(3) Martin, R. L.; Davidson, E. R. *Mol. Phys.* **1978**, *35*, 1713.

(4) Chapman, S. *Adv. Chem. Phys.* **1992**, *82*, 423.

(5) Osherov, V. I.; Ushakov, V. G. *Dokl. Akad. Nauk SSR* **1977**, *236*, 68 [English translation: *Sov. Phys. Dokl.* **1977**, *22*, 499].

(6) Blais, N. C.; Truhlar, D. G.; Mead, C. A. *J. Chem. Phys.* **1988**, *89*, 6204.

(7) Varandas, A. J. C.; Pais, A. A. C. C. *J. Chem. Soc. Faraday Trans.* **1993**, *89*, 1511.

(8) Pais, A. A. C. C.; Nalewajski, R. F.; Varandas, A. J. C. *J. Chem. Soc., Faraday Trans.* **1994**, *90*, 1381.

(9) Varandas, A. J. C. *Adv. Chem. Phys.* **1988**, *74*, 255.

(10) Varandas, A. J. C. *Chem. Phys. Lett.* **1992**, *194*, 333.

(11) Varandas, A. J. C.; Nalewajski, R. F. *Chem. Phys. Lett.* **1993**, *205*, 253.

(12) Thompson, T. C.; Izmirlian, Jr., G.; Lemon, S. J.; Truhlar, D. G.; Mead, C. A. *J. Chem. Phys.* **1985**, *82*, 5597.

(13) Varandas, A. J. C.; Morais, V. M. F.; Pais, A. A. C. C. *Mol. Phys.* **1986**, *58*, 285.

(14) Whitehead, J. C. *Mol. Phys.* **1976**, *31*, 549.

(15) Morais, V. M. F.; Varandas, A. J. C. *J. Chem. Soc., Faraday Trans. 2* **1989**, *85*, 1.

(16) Rubahn, H.-G. *J. Phys. Chem.* **1991**, *95*, 8215.

(17) Rubahn, H.-G.; Slenczka, A.; Toennies, J. P. *J. Chem. Phys.* **1994**, *101*, 1262.

(18) Morais, V. M. F.; Varandas, A. J. C. *Mol. Phys.* **1995**, *84*, 957.

(19) Pais, A. A. C. C.; Voronin, A. I.; Varandas, A. J. C. *J. Phys. Chem.* **1996**, *100*, 7480.

(20) Varandas, A. J. C.; Yu, H. G.; Xu, Z. R. *J. Chem. Phys.*, submitted for publication.

(21) Yarkony, D. R. *Rev. Mod. Phys.* **1996**, *68*, 985.

(22) Tully, J. C.; Preston, R. K. *J. Chem. Phys.* **1971**, *55*, 562.

(23) Tully, J. C. In *Modern Theoretical Chemistry, Dynamics of Molecular Collisions, Part B*; Miller, W. H.. Ed.; Plenum Press: New York, 1977; p 217.

(24) Osherov, V. I.; Ushakov, V. G. *Sov. Phys. Dokl.* **1977**, *22*, 499.

(25) Dehareng, D.; Chapuisat, X.; Lorquet, J. C.; Galloy, C.; Raseev, G. *J. Chem. Phys.* **1983**, *78*, 1246.

(26) Desouter-Lecomte, M.; Dehareng, D.; Leyh-Nihant, B.; Praet, M. Th.; Lorquet, A. J.; Lorquet, J. C. *J. Phys. Chem.* **1985**, *89*, 214.

(27) Last, I.; Baer, M. *J. Chem. Phys.* **1985**, *82*, 4954.

(28) Cattaneo, P.; Persico, M. *J. Phys. Chem. A* **1997**, *101*, 3454.

(29) Preston, R. K.; Tully, J. C. *J. Chem. Phys.* **1971**, *54*, 4297.

(30) Tully, J. C. *J. Chem. Phys.* **1990**, *93*, 1061.

(31) Tully, J. C. *Int. J. Quant. Chem. Symp.* **1991**, *25*, 299.

(32) Gislason, E. A. *Adv. Chem. Phys.* **1992**, *82*, 321.

(33) Smith, B. R.; Bearpark, M.; Robb, M. A.; Bernardi, F.; Olivucci, M. *Chem. Phys. Lett.* **1995**, *242*, 27.

(34) Muckerman, J. T. QCPE,# 229, Indiana University: Bloomington, IN, 1973.

(35) Sinha, M. P.; Schultz, A.; Zare, R. N. *J. Chem. Phys.* **1973**, *58*, 549.